Carbohydrate Polymers 80 (2010) 665–671

Contents lists available at ScienceDirect

Carbohydrate Polymers

journal homepage: www.elsevier.com/locate/carbpol

Role of starch nanocrystals and cellulose whiskers in synergistic reinforcement of waterborne polyurethane

Yixiang Wang, Huafeng Tian, Lina Zhang *

Department of Chemistry, Wuhan University, Wuhan 430072, China

ARTICLE INFO

Article history:
Received 15 July 2009
Received in revised form 12 October 2009
Accepted 16 October 2009
Available online 21 October 2009

Keywords:
Starch nanocrystals
Cellulose whiskers
Synergistic reinforcement
Waterborne polyurethane

ABSTRACT

Starch nanocrystals (SN) and cellulose whiskers (CW) were fabricated successfully from the sulfuric acid hydrolysis of waxy maize starch granules and cotton linter pulp, respectively, and were characterized by transmission electron microscopy, atomic force microscopy and wide-angle X-ray diffraction. The nanocrystals and whiskers were embedded in waterborne polyurethane (WPU) matrix using a casting/evaporation technique. A synergistic reinforcing role of SN and CW in WPU was observed for the first time. With incorporation of 1 wt.% SN and 0.4 wt.% CW, the tensile strength, Young's modulus and tensile energy at break of the WPU based nanocomposites were significantly enhanced by 135%, 252% and 136%, respectively, and the elongation at break remained basically compared to pure WPU. WPU/1% SN/0.4% CW system also exhibited a much better reinforcing effect than all of WPU/SN and WPU/CW systems. Furthermore, the WPU based nanocomposites possessed greater thermal resistance. The results clearly revealed that the different polysaccharide nanocrystals and whiskers combined together to form strong hydrogen bonding networks, leading to the synergistic reinforcement of WPU. This work provides a new eco-friendly pathway to prepare polymer nanocomposites with high performance by using natural nanocrystals and whiskers together.

1. Introduction

A possible source of inspiration for the design of new high performance materials is the nature and its wonderful nanocomposite structures (Habibi & Dufresne, 2008). Many living organisms have the ability to biosynthesize polymer crystals. During the last decade, a kind of novel nano-materials derived from natural polymers, named as "green" bionanocomposites (Darder, Aranda, & Ruiz-Hitzky, 2007), has been developed, in which natural polymers can act as the matrix, the nanofiller or both. Usually, natural nanofillers are the crystalline residue with a uniform structure after acidic or alkaline hydrolysis of natural polysaccharides. The crystalline nanoparticles from different sources have different geometrical characteristics, such as rod-like nanocrystals or whiskers of cellulose (van den Berg, Capadona, & Weder, 2007a) and chitin (Lu, Weng, & Zhang, 2004), and platelet-like nanocrystal of starch (Angellier, Choisnard, Molina-Biosseau, Ozil, & Dufresne, 2004). They have provided wide applications because of their potential nanoparticle properties. Many attempts have been reported to blend polysaccharide nanocrystals with polymeric matrices (Goetz, Mathew, Oksman, Gatenholm, & Ragauskas, 2009; Kristo & Biliaderis, 2007; Paralikar, Simonsen, & Lombardi, 2008; van den Berg, Schroeter, Capadona, & Weder, 2007b). The resulting nanocomposite materials display outstanding mechanical properties and thermal stability. For example, starch nanocrystals (SN) present the originality to consist of crystalline nanoplatelets about 6–8 nm thick with a length of 20–40 nm and a width of 15–30 nm (Labet, Thielemans, & Dufresne, 2007). They have been used as a new kind of fillers, showing interesting reinforcing and barrier properties in natural rubber (Angellier, Molina-Boisseau, Lebrun, & Dufresne, 2005a; Angellier, Molina-Boisseau, & Dufresne, 2005b). On the other hand, cellulose whiskers (CW) are considered to be an ideal loading-bearing constituent in developing new and inexpensive biodegradable materials due to their high aspect ratio, high bending strength of about 10 GPa and high Young's modulus of approximately 150 GPa (Sturcova, Davies, & Eichhorn, 2005).

Polyurethanes (PUs) are one of the most versatile polymeric materials with regard to both processing methods and mechanical properties (Lu & Larock, 2008). However, the conventional PU products usually contain a significant amount of organic solvents and sometimes even free isocyanate monomers (Modesti & Lorenzetti, 2001). Therefore, these solvent-based PUs have been gradually replaced by the waterborne polyurethanes (WPUs) in past decades because of the increasing need to reduce volatile organic compounds (VOCs) and hazardous air pollutants (HAPs) (Wicks, Wicks, & Rosthauser, 2002). WPUs present many advantages,

* Corresponding author. Tel.: +86 27 87219274; fax: +86 27 68754067.
E-mail addresses: lnzhang@public.wh.hb.cn, linazhangwhu@gmail.com (L. Zhang).

0144-8617/$ - see front matter © 2010 Published by Elsevier Ltd.
doi:10.1016/j.carbpol.2009.10.043

including non-toxic, non-flammable, non-pollution, low viscosity at high molecular weight and good applicability, and are now one of the most rapidly developing and active branches of PU chemistry and technology (Jeon, Jang, Kim, & Kim, 2007). Recently, a series of researches focus on the addition of nanosized particles, especially polysaccharide nanocrystals, in the WPU matrix to improve the thermal resistance and mechanical properties of WPU materials (Cao, Dong, & Li, 2007; Chen et al., 2008; Lee & Lin, 2006; Wu, Henriksson, Liu, & Berglund, 2007; Wang & Zhang, 2008). These novel materials are eco-friendly and biodegradable, which have a potential application in medical and biologic fields.

It is proved that the extent of the reinforcement depends on such factors as the dispersion of the nanofillers in the polymer matrix and the interfacial adhesion between nanofillers and polymer matrix (Nair & Dufresne, 2003). Few literatures have been reported on the nanofillers with different geometrical characteristics for improving the properties of polymer matrix (Tang et al., 2008; Zhang, Phang, & Liu, 2006). However, no report on using the natural nanocrystals and whiskers together as a reinforcing phase is observed. In the present work, we make a good effort to improve the mechanical properties and thermal stability of WPU by using both starch nanocrystals and cellulose whiskers simultaneously. Their morphology, structure and performance were investigated in detail by transmission electron microscopy, dynamic mechanical thermal analysis, thermogravimetric analysis and tensile testing to judge the reinforcing mechanism of these two fillers. This work may contribute some meaningful information for the application of polysaccharide nanocrystals in producing high performance polymeric materials.

2. Experimental

2.1. Materials

All of the chemical reagents used in this work were of analytically grade, and were purchased from commercial sources in China. Commercial waxy maize starch containing 0.5 wt.% protein, 0.15 wt.% fat and 0.15 wt.% ash was a gift of Gansu Xue Jing Biochemical Co., Ltd. (China). Cellulose (cotton linter pulp) was supplied by the Hubei Chemical Fiber Group, Ltd. 2,4-Toluene diisocyanate (TDI) was purchased from Jiangbei Chemical Reagents Factory (Wuhan, China). TDI was redistilled before use. Polypropylene glycol (PPG) having weight-average molecular weight (M_w) of 2000 was supplied by Sinopharm Chemical Reagent Co. Ltd., and vacuum-dried at 120 °C for 1 h before use. Dimethylol propionic acid (DMPA) was obtained from Chengdu Polyurethane Co. in China. Triethylamine (TEA), sulfuric acid and acetone were purchased from Shanghai Chemical Co. in China. TEA and acetone were treated with 3 Å molecular sieves to dehydrate. Starch and cellulose were vacuum-dried at 105 °C for 5 h before use.

2.2. Preparation of nanocrystals

Waxy maize starch granules (25 g) were mixed with 200 mL of 3.16 M sulfuric acid for 5 days at 40 °C, with a stirring speed of 100 rpm. Then the suspension was diluted with distilled water, and then centrifuged (10,000 rpm for 15 min). The process was repeated three times to wipe off the excess sulfuric acid. The resultant suspension, which had a weight concentration of about 5 wt.%, was treated with ultrasonic. Then, it was freeze-dried to obtain starch nanocrystal powder (SN) (Wang & Zhang, 2008).

Cotton linter pulp (20 g) was dispersed in 175 mL of a 30% (v/v) sulfuric acid, and the mixture was added to a three-necked flask equipped with a mechanical stirrer and a thermometer. The flask was placed into a water bath at 60 °C and stirred vigorously for 6 h. The suspension was then diluted with distilled water, and centrifuged at 8000 rpm for 15 min. The process was repeated three times to remove the excess sulfuric acid. The resulting suspension was dialyzed for 2 h in running water and then overnight in distilled water, until the pH reached 4. Finally, the dispersion was treated with ultrasonic, and freeze-dried to obtain cellulose whisker powder (CW) (Wang, Cao, & Zhang, 2006).

2.3. Processing of nanocomposite films

PPG2000 (116 g, 0.058 mol) and DMPA (2.68 g, 0.02 mol) were introduced into a four-neck flask equipped with a thermometer, mechanical stirrer, dropping funnel, and condenser, and the mixture was heated to 80 °C; then TDI (20 g, 0.111 mol) was added dropwise, and the reaction was carried out in dry nitrogen atmosphere for 2–3 h until the –NCO content reached a desired value, which was determined by using the standard dibutylamine titration method. Subsequently, 30 g acetone was poured into the flask to reduce the viscosity of prepolymer and then cooled to 60 °C. After neutralization of carboxylic groups of DMPA with TEA (2.1 g, 0.02 mol) for 30 min, the product was dispersed with distilled water under vigorous stirring. After the mixture was stirred at room temperature overnight, the acetone was removed by rotary vacuum evaporating at 30 °C, and the solid content of the WPU was 20 wt.% finally.

SN and CW were firstly dispersed in distilled water and ultrasonicated for 15 min to avoid the aggregations. Then, the suspensions of nanocrystals and WPU were mixed with SN content ranging from 1 to 5 wt.% and CW content from 0.2 to 1 wt.% (with respect to WPU), followed by stirring for 5 h. Subsequently, the resulting mixtures were degassed for 3 h under vacuum. Nanocomposite films with a mean thickness of 0.2 mm were prepared by drying the mixtures in some hydrophobic glass plates at room temperature for 2 weeks. Before various characterizations, the films were conditioned at room temperature in a desiccators containing P_2O_5 with 0% relative humidity (RH).

2.4. Characterizations

Transmission electron microscope (TEM) observation of the morphology of SN and the nanocomposite film was carried out on a JEM-2010 TEM (JEOL TEM, Japan). SN were dispersed in distilled water and ultrasonicated for 15 min. Then, a small droplet of the dilute suspension was deposited on a polycarbon film, which was supported on a copper grid. A thin layer was suspended over the holes of the grid. The specimen was dried in air at ambient pressure, and then was imaged on TEM at an accelerating voltage of 200 kV. The film was cut into thin strips with the cross-section of about 0.2–0.3 mm^2. They were embedded in Epon 812 epoxy resin and cured at 40 °C for 60 h. The embedded specimens were first trimmed with a razor blade and then with an ultra-cut microtome equipped with a glass knife. An extremely smooth trapezoidal top surface was obtained with the cross-section of the polymer strip. ALKBIII microtome was used for ultra-thin microtomy. The top layer (about 1 mm) was first removed using a glass knife, then, ultra-thin sections of about 100 nm thickness were cut with a Diatome diamond knife at room temperature. The ultra-thin sections were stained by OsO_4 and mounted on 200 mesh copper grids for TEM observation.

Atomic force microscopy (AFM) analysis of CW in suspension was carried out on an XE-100 microscope (PSIA Co., Korea). A droplet of the dilute CW suspension was coated onto a flake of mica, and the water was evaporated at room temperature for 24 h. Wide-angle X-ray diffraction patterns were recorded on X-ray diffraction (XRD-6000, Shimadzu, Japan), using Cu Kα radiation (λ = 0.154 nm) at 40 kV and 30 mA with a scan rate of 1°/min.

Dynamic mechanical thermal analysis (DMTA) was performed on a dynamic mechanical analyzer (DMA Q800, TA Instruments, USA) in tensile mode at a frequency of 1 Hz. The films were 10 mm × 10 mm (length × width) in dimension, and the test temperature ranged from −70 to 80 °C, with a heating rate of 5 °C per min. The α-relaxation temperature, T_α, was determined as the peak value of the loss angle tangent (tan δ). A thermogravimetric analyzer (TGA Q500, TA Instruments, USA) was used to measure the weight losses of the nanocomposite films in the temperature range from 40 to 500 °C with a heating rate of 10 °C/min and under an argon stream. The tensile strength (σ_b), elongation at break (ε_b), and the Young's modulus (E) of the nanocomposite films were measured on a universal testing machine (CMT6503, Shenzhen SANS Test Machine Co. Ltd., Shenzhen, China) with a tensile rate of 50 mm per min at 25 ± 2 °C according to ISO527-3: 1995(E). Before testing, the films were allowed to rest for one week in 0% RH. Five parallel measurements were carried out for each sample.

3. Results and discussion

TEM image of the dilute suspension of SN is shown in Fig. 1. Although the SN tended to self-aggregate, the distinguished isolated SN having the width of 15–25 nm and the length of 35–50 nm were observed, in agreement with the report in the literature (Putaux, Molina-Boisseau, Momaur, & Dufresne, 2003). AFM image of a dilute suspension of CW was shown in Fig. 2. The individual cellulose whiskers in the aqueous suspension displayed slender rods and had a narrow distribution in size. They had lengths (L) ranging from 700 to 800 nm and widths (D) ranging from 80 to 100 nm. Therefore, the average aspect ratio, L/D, was 8.5, which was smaller than the reported value (Wang et al., 2006). It indicated that the treatment of the cotton linter pulp with acid, sodium hydroxide and sodium hypochlorite during the production process had an extent of effect on the morphology of CW. SN and CW exhibited the quite different geometrical characteristics, implying their different reinforcing behaviors. At the same time, their similar molecular structures and good compatibility provided a possibility of synergistic reinforcing effect to use together. Fig. 3 shows the wide-angle X-ray diffraction patterns of both SN and CW. Native starch is a kind of semicrystalline polymer.

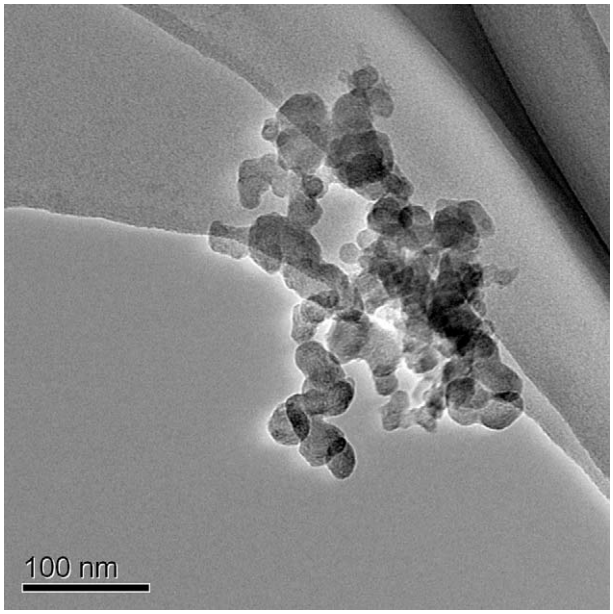

Fig. 1. TEM image of dilute suspension of starch nanocrystals.

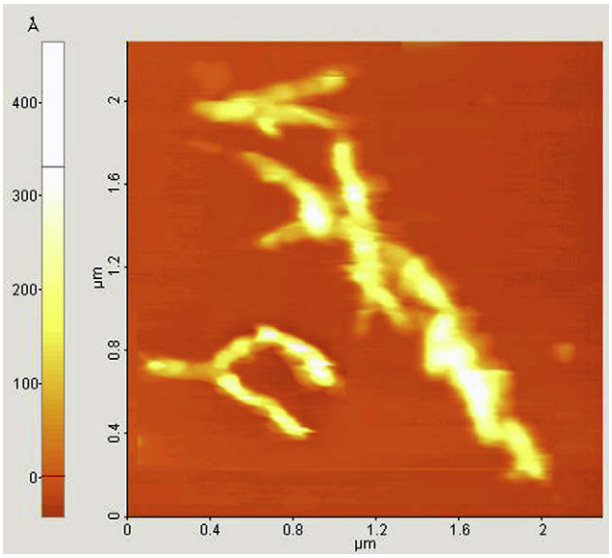

Fig. 2. AFM topography image of cellulose whiskers after drying on a mica surface.

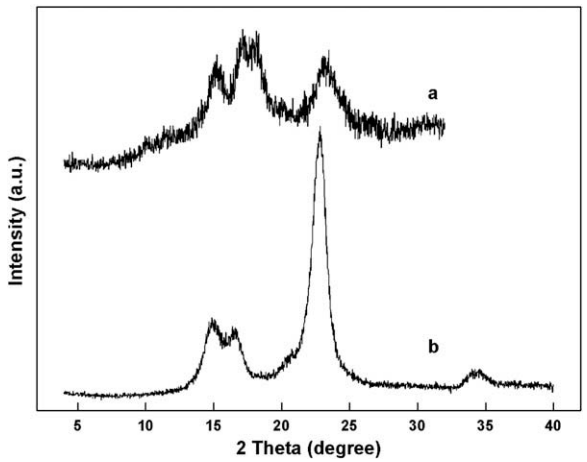

Fig. 3. X-ray diffraction patterns of starch nanocrystals (a) and cellulose whiskers (b).

There were two weak peaks at $2\theta = 10.1°$ (0.87 nm) and 11.5° (0.76 nm), a strong peak at 15.3° (0.57 nm), a double strong peak at 17.1° (0.52 nm) and 18.2° (0.49 nm), and a strong peak at 23.5° (0.39 nm) in the diffraction pattern for SN, displayed typical peaks of A-type crystalline (Buléon, Gérard, Riekel, Vuong, & Chanzy, 1998). Meanwhile, CW displayed four well-defined diffraction peaks at 14.8° (0.60 nm), 16.5° (0.54 nm), 22.6° (0.39 nm), and 34.5° (0.258 nm), which were typical of cellulose I (Nishiyama, Langan, & Chanzy, 2002).

Fig. 4 shows the mechanical properties of WPU and its nanocomposites. The unique synergistic effect of SN and CW on the reinforcing of WPU was observed. For both WPU/SN and WPU/CW binary nanocomposite films, the tensile strength increased with the nanofiller content as shown in Fig. 4a and b. The increase of tensile strength was most obvious at 1 wt.% SN for WPU/SN and 0.4 wt.% CW for WPU/CW. With a further addition of nanofiller content, the mechanical properties of binary nanocomposite films dropped due to the formation of aggregation of the nanofillers (Wang & Zhang, 2008). To avoid the aggregation and utilize the different geometrical characteristics of SN and CW, they were used together and a dramatic increase of tensile strength of WPU was observed as expected. The tensile strengths of WPU/SN/CW ternary

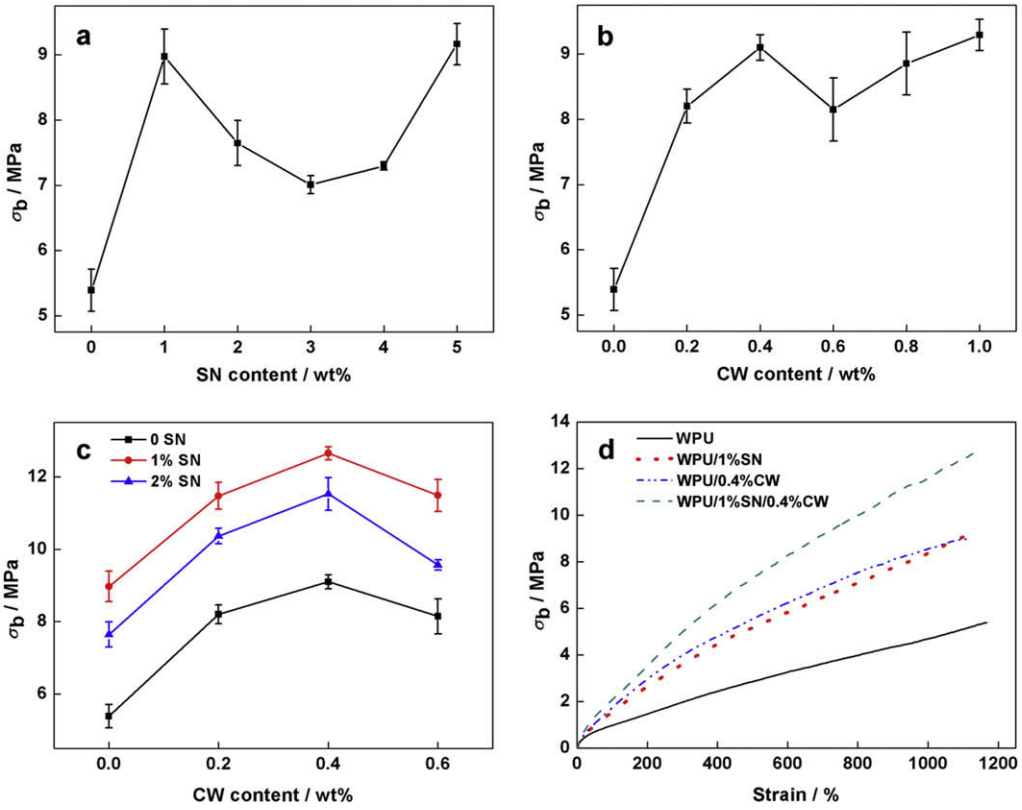

Fig. 4. (a) Dependence of tensile strength (σ_b) of WPU/SN nanocomposite films on SN content; (b) dependence of tensile strength of WPU/CW nanocomposite films on CW content; (c) dependence of tensile strength of WPU/SN/CW nanocomposite films on CW content; (d) stress–strain curves of pure WPU, WPU/1% SN, WPU/0.4% CW, and WPU/1% SN/0.4% CW nanocomposite films.

Table 1
Tensile and thermal properties of pure WPU and its nanocomposite films.

Samples	Young's modulus (MPa)	Tensile strength (MPa)	Elongation at break (%)	Tensile energy (MJ m^{-3})	T_α (°C)	30% Weight loss temperature (°C)
WPU	0.5 ± 0.1	5.4 ± 0.3	1167 ± 8.9	35.8 ± 2.0	−24.3	305.2
WPU/1% SN	1.0 ± 0.1	9.1 ± 0.2	1106 ± 24.3	58.2 ± 1.3	−27.4	322.3
WPU/0.4% CW	1.2 ± 0.2	9.0 ± 0.4	1119 ± 27.4	62.8 ± 2.8	−26.0	339.1
WPU/1% SN/0.4% CW	1.8 ± 0.3	12.7 ± 0.2	1133 ± 12.2	84.6 ± 1.4	−25.5	353.9

nanocomposite films as function of CW content are shown in Fig. 4c. The CW content varied from 0 to 0.6 wt.%, and the SN content ranged from 0 to 2 wt.%. It was worth noting that the tensile strengths of WPU/SN/CW systems were higher than those of all the WPU/SN and WPU/CW systems, suggesting a synergistic reinforcing effect. When the CW content was 0.4 wt.%, the tensile strength of the ternary nanocomposite films reached the maximum value in different fraction of SN. The insertion of CW into the WPU/SN network produced a much jammed structure combined by hydrogen bond (Kondo, Koschella, Heublein, Klemm, & Heinze, 2008), which largely enhanced the tensile strength of WPU. The results indicated that a proper jammed network formed when the SN content was 1 wt.% and the CW content was 0.4 wt.%. Typical stress–strain curves of pure WPU and its nanocomposite films are shown in Fig. 4d. Their mechanical properties are summarized in Table 1. The tensile energy at break is calculated by the areas below the stress–strain curves, which is relative to the toughness of samples. Clearly, with incorporation of both SN (1 wt.%) and CW (0.4 wt.%), the tensile strength of the nanocomposite films was increased from 5.4 to 12.7 MPa, Young's modulus was increased from 0.5 to 1.8 MPa, and the tensile energy at break was increased from 35.8 to 84.6 MJ m^{-3}, compared to pure WPU. All the tensile strength, Young's modulus and tensile energy at break of WPU/1% SN/0.4% CW nanocomposite films were much higher than those corresponding binary nanocomposite films WPU/1% SN (9.1 and 1.0 MPa, 58.2 MJ m^{-3}) or WPU/0.4% CW (9.0 and 1.2 MPa, 62.8 MJ m^{-3}). Interestingly, the ternary system displayed a similar elongation at break compared to pure WPU, which was relatively higher than those of binary systems. This could be explained that the much jammed hydrogen bonding networks occurred in the ternary nanocomposite films, because of the large specific surface of SN and rod-like shape of CW. The load fastened on the nanocomposite films would be transmitted to the network and dispersed speedily (Pan & Chen, 2007). To confirm the morphology of the nanocomposite film, TEM image of the ultra-thin sections of WPU/1% SN/0.4% CW film is shown in Fig. 5a. The result exhibited the existence of individual SN and CW, and no big aggregates were observed. It indicated that the nanofillers were uniformly dispersed in WPU matrix during the solution mixing process. It is well known that intermolecular hydrogen bonds can occur between polysaccharide nanocrystals and WPU matrix (Chen et al., 2008). The geometrical characteristics of SN were all under

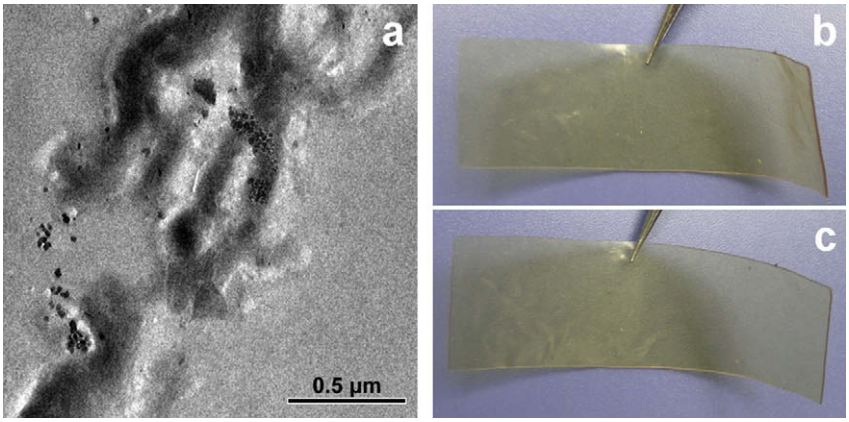

Fig. 5. TEM image of ultra-thin section of WPU/1% SN/0.4% CW nanocomposite films (a), and photographs of WPU (b) and WPU/1% SN/0.4% CW (c).

100 nm, so the interactions between SN and WPU existed and SN became the crosslinking points of the networks, leading to the reinforcement of WPU matrix. At the meantime, CW was rod-like nanocrystal and can insert into the WPU/SN networks as observed in Fig. 5a. CW located in SN platelets regions and connected with SN to form a new type of SN–CW networks. This jammed nanofillers networks were found, for the first time, and they played an important role in reinforcing the WPU matrix, supported by the results in Fig. 4. Interestingly, the formation of new networks did not affect the appearance of WPU and its nanocomposite films as shown in Fig. 5b and c, indicating the uniform dispersion of the nanofillers in the WPU matrix.

DMTA test, a technique sensitive to molecular movement, was carried out to further understand the unique synergistic effect of SN and CW on the reinforcing of WPU. Fig. 6 shows the temperature dependence of the loss peaks (tan δ) and the storage modulus (E') of pure WPU and its nanocomposite films. The T_α values were assigned to the glass-rubber transition of the soft segments of the WPU matrix, and the results are summarized in Table 1. Actually, the addition of nanofillers could influence the values of T_α in two opposite ways. In one aspect, the solid surface of polysaccharide nanocrystals could induce a restricted mobility of WPU chains by forming hydrogen bonds both between the nanofillers and between the nanofillers and the hard segments of WPU. It could result in an increase of the physical crosslink density and a shift of T_α toward higher temperature; in another, the strong interactions between the nanofillers and the hard segments might improve the microphase separation in WPU. This effect could result in a decrease of T_α of the soft segment indirectly. In our findings, the downward trend of T_α of the nanocomposite films could be attributed to the improvement of the degree of freedom for the soft segment in WPU, as a result of an improvement of microphase separation in WPU caused by the strong hydrogen bonding between the nanofillers and the hard segments. Interestingly, the value of T_α of the ternary system was higher than those of binary systems, indicating that stronger hydrogen bonding interaction existed due to the formation of much jammed network, which well supported the results of tensile testing.

The addition of nanofillers increased the modulus of WPU, especially, the plateau modulus, suggesting a good reinforcement in WPU matrix. The drop in E' of the nanocomposite films at T_α was therefore ascribed to energy dissipation phenomena involving cooperative motions of long amorphous sequences likely to rotate and translate in different surroundings (Lu, Tighzert, Dole, & Erre, 2005). It is well known that the value of E' at the rubbery plateau can be used to estimate crosslink density of the polymer network (Pan & Chen, 2007). As shown in Fig. 6, the rubbery plateau modulus of pure WPU and its nanocomposite films decreased with the increase of temperature, which was different from that of ideal rubber. It was the result of that the hydrogen bonding interactions in WPU matrix and both between the nanofillers and between the nanofillers and the hard segments of WPU might partly dissociate with increasing temperature.

The physical crosslink density in WPU can be expressed in a manner as the following equation (Weisfeld, Little, & Wolstenholme, 1962):

$$\upsilon s/V = A\exp(E_a/RT) \quad (1)$$

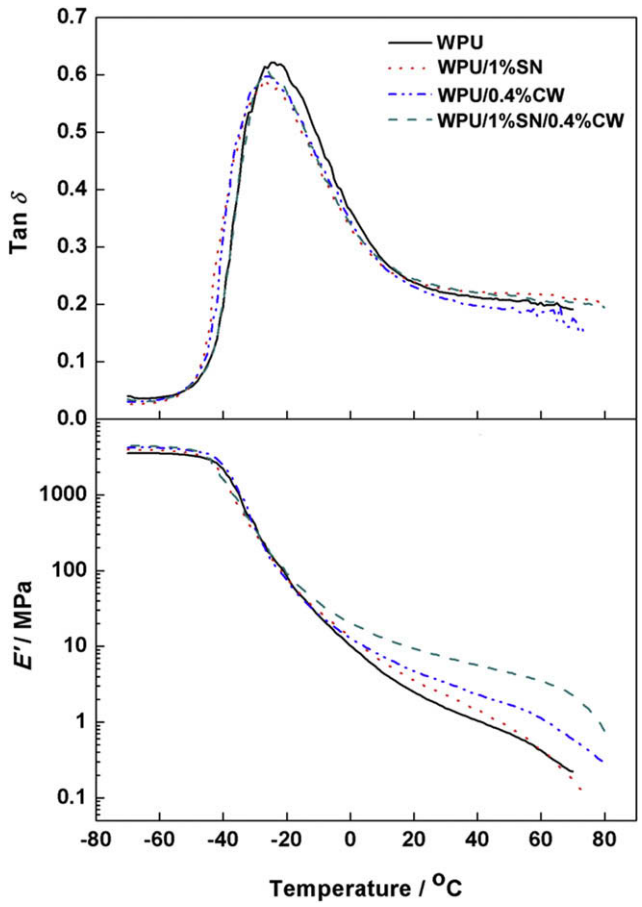

Fig. 6. Temperature dependence of the storage modulus (E') and loss peaks (tan δ) of pure WPU and its nanocomposite films.

where vs/V is the physical crosslinking density, A is a constant, R is the gas constant, T is the absolute temperature, and E_a is the apparent activation energy of hydrogen bonding dissociation. According to the kinetic theory of elasticity, the plateau modulus can be expressed as the following equation:

$$E' = (vs/V)RT = ART\exp(E_a/RT) \quad (2)$$

Eq. (2) can be rewriting as:

$$\ln E'/T = \ln AR + E_a/RT \quad (3)$$

Thus, E_a and A can be obtained from the slope and intersection of the straight line by plotting of $\ln E'/T$ versus $1/T$, as shown in Fig. 7. The values of E_a calculated from the slope of the straight line were 37.3 kJ/mol for WPU, 37.1 kJ/mol for WPU/1% SN, 30.7 kJ/mol for WPU/0.4% CW, and 22.3 kJ/mol for WPU/1% SN/0.4% CW, respectively. The physical crosslink density, vs/V, can be calculated by Eq. (1), as shown in Fig. 8. The values of vs/V increased with the addition of polysaccharide nanocrystals in the plateau temperature region, and that of the ternary system was much higher than others'. It clearly indicated that a much jammed hydrogen bonding networks formed as a result of the introduction of both SN and CW in the WPU matrix.

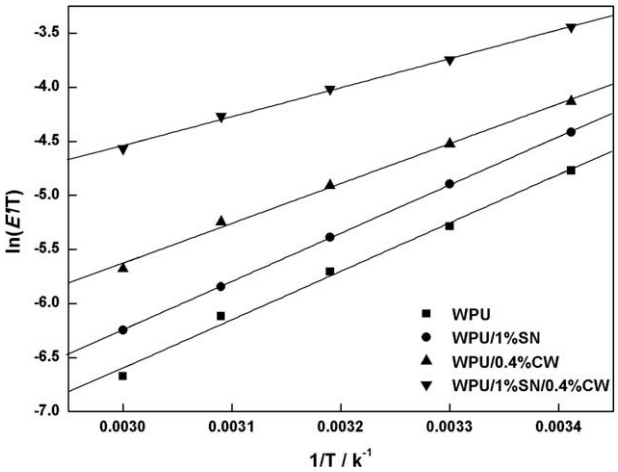

Fig. 7. Relationship between $\ln E'/T$ and $1/T$.

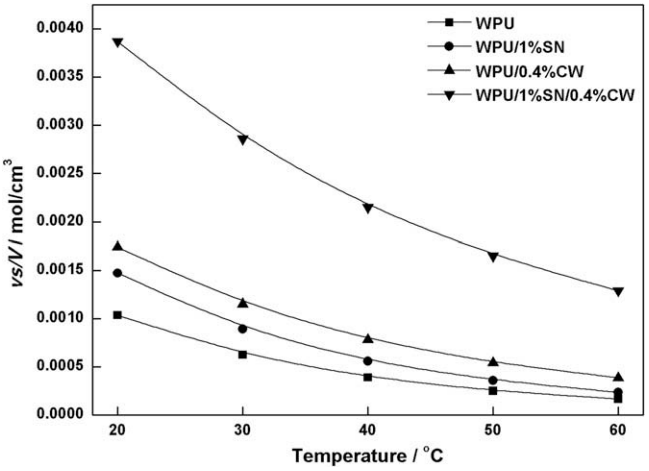

Fig. 8. Temperature dependence of physical crosslink density (vs/V) of pure WPU and its nanocomposite films.

Fig. 9 shows the results of TGA measurement for pure WPU and its nanocomposite films. The thermal degradation temperatures of 30% weight loss are listed in Table 1. Obviously, there was a two-step weight loss process for all the samples, associated to the earlier decomposition of the hard segment and the later decomposition of the soft segment, respectively. The films containing polysaccharide nanocrystals, especially the ternary system, exhibited higher thermal resistance than pure WPU. The temperature of 30% weight loss was enhanced from 305.2 to 353.9 °C. It was worth noting that the addition of nanofillers displayed a more distinct effect on improving the thermal resistance of the hard segment, while the rate of the thermal decomposition of the soft segment was even faster than that of pure WPU. This could be explained that strong hydrogen bonding interactions existed between the nanofillers and the hard segments, especially in the ternary system; at the mean while, these interactions induced the microphase separation between the hard and soft segments, leading to the acceleration of the decomposition of the soft segments. This result was also consistent with that of DMTA test.

On the basis of the results discussed above, a schematic description of the morphology of pure WPU and SN and CW in WPU matrix is proposed in Fig. 10. In the pure WPU matrix (Fig. 10a), the physical crosslink density was relatively low. The jammed hydrogen bonding networks of polysaccharide nanocrystals and whiskers formed in the nanocomposite films, causing the synergistic reinforcement of the WPU matrix. SN acted as the crosslinking points of the networks, while CW provided strong effects of connection and sustentation as shown in Fig. 10b. Thus, the mechani-

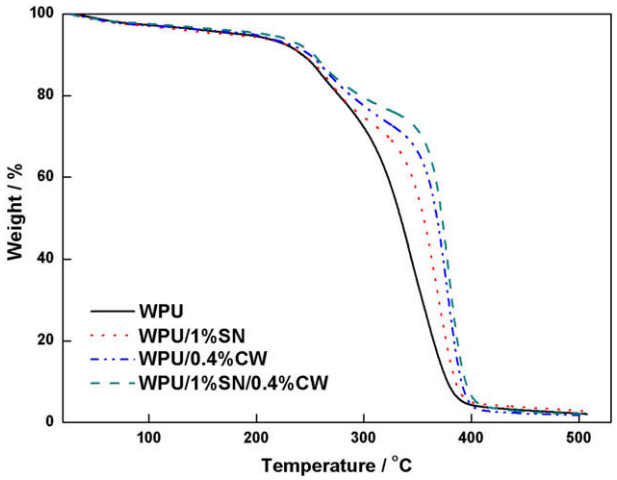

Fig. 9. TGA curves of pure WPU and its nanocomposite films.

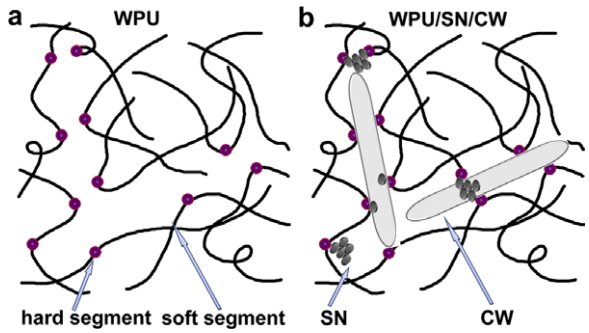

Fig. 10. Schematic illustration of pure WPU matrix (a) and jammed networks of SN and CW in WPU matrix (b).

cal properties and thermal resistance of WPU were dramatically improved. Furthermore, the strong interactions between the nanofillers and the matrix induced the microphase separation in WPU, leading to the little downward trends of elongation at break and T_α, and the faster decomposition of the soft segment of the nanocomposite films.

4. Conclusions

Polysaccharide nanocrystals fabricated from waxy maize starch and cotton linter pulp were used together to prepare WPU based nanocomposite films with high performance successfully. A great synergistic effect of SN and CW on reinforcing the WPU matrix has been observed. With incorporation of 1 wt.% SN and 0.4 wt.% CW, the tensile strength, Young's modulus and tensile energy at break of the nanocomposites were significantly improved by 135%, 252% and 136%, respectively, and the elongation at break remained basically compared to pure WPU. WPU/1% SN/0.4% CW system also exhibited a much better reinforcing effect, compared to all of WPU/SN and WPU/CW systems. In the ternary system, the formation of much jammed network consisted of nanocrystals and whiskers with different geometrical characteristics from polysaccharides played an important role in the enhancement of the crosslink networks. Strong hydrogen bonding interactions existed both between the nanofillers and between the nanofillers and the hard segments of WPU matrix, leading to the improvement of the mechanical and thermal properties. This work provided important information that utilizing nanocrystals and whiskers together can increase the density of the networks, so as to improve the performance of the materials. More novel green bionanocomposite materials with superior mechanical properties could be expected by introducing the natural nanocrystals with different geometrical characteristics together.

Acknowledgments

This work was supported by the major grant of the National Natural Science Foundation of China (30530850, 20874079 and 20474048), and the National Support Project for Science and Technology (2006BAF02A09).

References

Angellier, H., Choisnard, L., Molina-Biosseau, S., Ozil, P., & Dufresne, A. (2004). Optimization of the preparation of aqueous suspensions of waxy maize starch nanocrystals using a response surface methodology. *Biomacromolecules, 5*, 1545–1551.

Angellier, H., Molina-Boisseau, S., Lebrun, L., & Dufresne, A. (2005a). Processing and structural properties of waxy maize starch nanocrystals reinforced natural rubber. *Macromolecules, 38*, 3783–3792.

Angellier, H., Molina-Boisseau, S., & Dufresne, A. (2005b). Mechanical properties of waxy maize starch nanocrystal reinforced natural rubber. *Macromolecules, 38*, 9161–9170.

Buléon, A., Gérard, C., Riekel, C., Vuong, R., & Chanzy, H. (1998). Details of the crystalline ultrastructure of C-starch granules revealed by synchrotron microfocus mapping. *Macromolecules, 31*, 6605–6610.

Cao, X., Dong, H., & Li, C. (2007). New nanocomposite materials reinforced with flax cellulose nanocrystals in waterborne polyurethane. *Biomacromolecules, 8*, 899–904.

Chen, G., Wei, M., Chen, J., Huang, J., Dufresne, A., & Chang, P. R. (2008). Simultaneous reinforcing and toughening: New nanocomposites of waterborne polyurethane filled with low loading level of starch nanocrystals. *Polymer, 49*, 1860–1870.

Darder, M., Aranda, P., & Ruiz-Hitzky, E. (2007). Bionanocomposites: A new concept of ecological, bioinspired, and functional hybrid materials. *Advanced Materials, 19*, 1309–1319.

Goetz, L., Mathew, A., Oksman, K., Gatenholm, P., & Ragauskas, A. J. (2009). A novel nanocomposite film prepared from crosslinked cellulosic whiskers. *Carbohydrate Polymers, 75*, 85–89.

Habibi, Y., & Dufresne, A. (2008). Highly filled bionanocomposites from functionalized polysaccharide nanocrystals. *Biomacromolecules, 9*, 1974–1980.

Jeon, H. T., Jang, M. K., Kim, B. K., & Kim, K. H. (2007). Synthesis and characterizations of waterborne polyurethane–silica hybrids using sol–gel process. *Colloids and Surfaces A: Physicochemical and Engineering Aspects, 302*, 559–567.

Kondo, T., Koschella, A., Heublein, B., Klemm, D., & Heinze, T. (2008). Hydrogen bond formation in regioselectively functionalized 3-mono-*O*-methyl cellulose. *Carbohydrate Research, 343*, 2600–2604.

Kristo, E., & Biliaderis, C. G. (2007). Physical properties of starch nanocrystal-reinforced pullulan films. *Carbohydrate Polymers, 68*, 146–158.

Labet, M., Thielemans, W., & Dufresne, A. (2007). Polymer grafting onto starch nanocrystals. *Biomacromolecules, 8*, 2916–2927.

Lee, H., & Lin, L. (2006). Waterborne polyurethane/clay nanocomposites: Novel effects of the clay and its interlayer ions on the morphology and physical and electrical properties. *Macromolecules, 39*, 6133–6141.

Lu, Y., Weng, L., & Zhang, L. (2004). Morphology and properties of soy protein isolate thermoplastics reinforced with chitin whiskers. *Biomacromolecules, 5*, 1046–1051.

Lu, Y., Tighzert, L., Dole, P., & Erre, D. (2005). Preparation and properties of starch thermoplastics modified with waterborne polyurethane from renewable resources. *Polymer, 46*, 9863–9870.

Lu, Y., & Larock, R. C. (2008). Soybean-oil-based waterborne polyurethane dispersions: Effects of polyol functionality and hard segment content on properties. *Biomacromolecules, 9*, 3332–3340.

Modesti, M., & Lorenzetti, A. (2001). An experimental method for evaluating isocyanate conversion and trimer formation in polyisocyanate–polyurethane foams. *European Polymer Journal, 37*, 949–954.

Nair, K. G., & Dufresne, A. (2003). Crab shell chitin whisker reinforced natural rubber nanocomposites. 1. Processing and swelling behavior. *Biomacromolecules, 4*, 657–665.

Nishiyama, Y., Langan, P., & Chanzy, H. (2002). Crystal structure and hydrogen-bonding system in cellulose I_β from synchrotron X-ray and neutron fiber diffraction. *Journal of the American Chemical Society, 124*, 9074–9082.

Pan, H., & Chen, D. (2007). Preparation and characterization of waterborne polyurethane/attapulgite nanocomposites. *European Polymer Journal, 43*, 3766–3772.

Paralikar, S. A., Simonsen, J., & Lombardi, J. (2008). Poly(vinyl alcohol)/cellulose nanocrystal barrier membranes. *Journal of Membrane Science, 320*, 248–258.

Putaux, J. L., Molina-Boisseau, S., Momaur, T., & Dufresne, A. (2003). Platelet nanocrystals resulting from the disruption of waxy maize starch granules by acid hydrolysis. *Biomacromolecules, 4*, 1198–1202.

Sturcova, A., Davies, G. R., & Eichhorn, S. J. (2005). Elastic modulus and stress-transfer properties of tunicate cellulose whiskers. *Biomacromolecules, 6*, 1055–1061.

Tang, C., Xiang, L., Su, J., Wang, K., Yang, C., Zhang, Q., et al. (2008). Largely improved tensile properties of chitosan film via unique synergistic reinforcing effect of carbon nanotube and clay. *The Journal of Physical Chemistry B, 112*, 3876–3881.

van den Berg, O., Capadona, J. R., & Weder, C. (2007a). Preparation of homogeneous dispersions of tunicate cellulose whiskers in organic solvents. *Biomacromolecules, 8*, 1353–1357.

van den Berg, O., Schroeter, M., Capadona, J. R., & Weder, C. (2007b). Nanocomposites based on cellulose whiskers and (semi)conducting conjugated polymers. *Journal of Materials Chemistry, 17*, 2746–2753.

Wang, Y., Cao, X., & Zhang, L. (2006). Effects of cellulose whiskers on properties of soy protein thermoplastics. *Macromolecular Bioscience, 6*, 524–531.

Wang, Y., & Zhang, L. (2008). High-strength waterborne polyurethane reinforced with waxy maize starch nanocrystals. *Journal of Nanoscience and Nanotechnology, 8*, 5831–5838.

Weisfeld, L. B., Little, J. R., & Wolstenholme, W. E. (1962). Bonding in urethane elastomers. *Journal of Polymer Science, 56*, 455–463.

Wicks, Z. W., Wicks, D. A., & Rosthauser, J. W. (2002). Two package waterborne urethane systems. *Progress in Organic Coatings, 44*, 161–183.

Wu, Q., Henriksson, M., Liu, X., & Berglund, L. (2007). A high strength nanocomposite based on microcrystalline cellulose and polyurethane. *Biomacromolecules, 8*, 3687–3692.

Zhang, W. D., Phang, I. Y., & Liu, T. X. (2006). Growth of carbon nanotubes on clay: Unique nanostructured filler for high-performance polymer nanocomposites. *Advanced Materials, 18*, 73–77.